Journal of Materials Chemistry C

Accepted Manuscript

This article can be cited before page numbers have been issued, to do this please use: S. Huang, Y. Wu, F. Zeng, L. Sun and S. Wu, *J. Mater. Chem. C*, 2016, DOI: 10.1039/C6TC03116A.

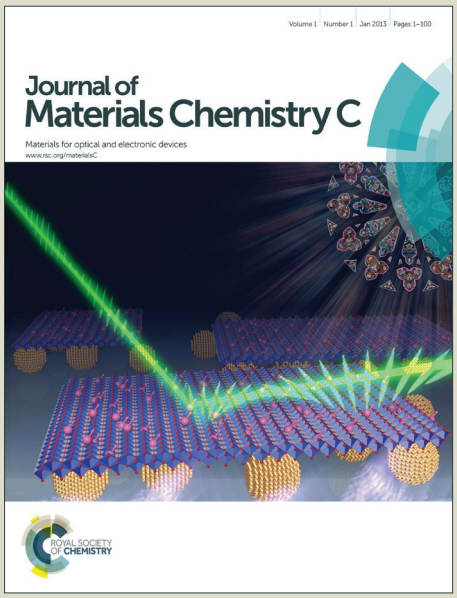

ROYAL SOCIETY OF CHEMISTRY

www.rsc.org/materialsC

View Article Online
DOI: 10.1039/C6TC03116A

Journal Name

ARTICLE

Handy ratiometric detection of gaseous nerve agents with AIE-fluorophore-based solid test strips

Received 00th January 20xx,
Accepted 00th January 20xx

DOI: 10.1039/x0xx00000x

www.rsc.org/

Shuailing Huang‡, Yinglong Wu‡, Fang Zeng*, Lihe Sun, Shuizhu Wu*

Exposure to the odorless, colorless, tasteless and yet lethal nerve gases could lead to paralysis of the central nervous system, organ failure or even rapid death. Hence it is of great importance to develop a convenient, portable and rapid detection method for these gaseous nerve agents. Herein, based on the aggregation-induced emission (AIE) characteristics, a ratiometric fluorescent test-strip sensor (DPA-TPE-Py) for rapid, sensitive and selective detection of gaseous nerve agent simulant --- diethyl chlorophosphate (DCP) has been developed. It is easy to prepare the handy and portable solid test strips via direct deposition of AIE probes onto the filter paper. Moreover, when exposed to DCP vapor, the fluorescence of the test strips changes from yellow to orange red. The detection limit for DCP is as low as 1.82 ppb, lower than the reported Immediately Dangerous to Life or Health concentration (IDLH concentration). Such a strategy could provide helpful insights on designing convenient cost-effective ratiometric fluorescent sensors in solid state as well as affording a portative method for detection of gaseous nerve agents.

Introduction

Chemical warfare agents (CWAs) are inclusive of nerve agents, blood agents, vesicant agents, incapacitating agents, asphyxiant agents, cytotoxic proteins and etc[1]. Among CWAs, nerve agents are extremely hazardous species by reason of their cheap and simple fabrication, possible use in offensive ways against military and civilian targets by terrorists, and extremely poisonous effects on human and animal health via inhalation or consumption of contaminated liquids or foods[2,3]. Chemically, nerve agents, such as Sarin (GB), Soman (GD), and Tabun (GA), are highly toxic organophosphates (OPs), whose reactive phosphate groups are able to irreversibly react with the hydroxyl groups of acetylcholinesterase (AChE, a critical enzyme responsible for the hydrolysis of acetylcholine neurotransmitter), thus blocking the decomposition of acetylcholine and resulting in the neurological imbalance in the cholinergic synapse, the paralysis of the central nervous system, organ failure and even rapid death[4,5]. The horrible threat of nerve agents to national and global security due to these agents' easy administration in terrorist attacks and their similar chemical structure to agricultural pesticides and herbicides, has posed the exigent need to detect these odorless, colorless, tasteless and yet lethal nerve agents[6]. In addition, the strong volatility of nerve agents and their usual deployment as the aerosol[2], underscores the sensitive, operationally facile, portable, low-cost detection of gas-phase nerve agents, as well as warning, pinpointing and tracking the perilous gases. Owing to the highly toxicity and unavailability of the real nerve agents, a related compound, diethyl chlorophosphate (DCP), is normally used as nerve-gas-mimic for scientific research, as it has the similar reactivity/structure[7]. A variety of detection methods have been studied and developed hitherto, including mass spectrometry, ion mobility spectrometry, enzyme-based biosensors and electrochemical sensors, which usually suffer from such limitations as non-portability, slow response, low sensitivity, lack of specificity and inconvenience in real-time detection resulting in their limited application in some conditions[7-9]. As an alternative to these detection methods, the easy-to-use fluorometric probes, which affords altered color or fluorescence emission, has proved feasible for detection[10-16] in different media with the advantages of operational simplicity, high sensitivity, low cost and real-time response[17-23]. Among them, dual-emission ratiometric fluorescent probes, based on the fluorescence intensity ratio of the reference and probe fluorophores at two different wavelengths, are of appreciated interest since they permit more accurate and precise analysis over the turn-on or turn-off probes by self-calibration at two emission bands[24].

To date, most of the fluorescent probes for detecting nerves agents have been designed to function in solution[25-27]. Compared with the liquid sensors, the membrane, sheet or strip sensors, which are easier to be incorporated into devices[28] and can contact more fully with the gas, are much more advantageous for gas detection. However, the current

College of Materials Science and Engineering, State Key Laboratory of Luminescent Materials and Devices, South China University of Technology, Guangzhou 510640, P. R. China.
E-mail: mcfzeng@scut.edu.cn, shzhwu@scut.edu.cn;
Fax: +86 20 22236363; Tel: +86 20 22236262
‡ These authors contributed equally to this work.
Electronic Supplementary Information (ESI) available: synthetic route, ^{1}H NMR and ^{13}C NMR spectra, mass spectra, absorption spectra, fluorescence lifetimes, and determination of detection limit. See DOI: 10.1039/x0xx00000x

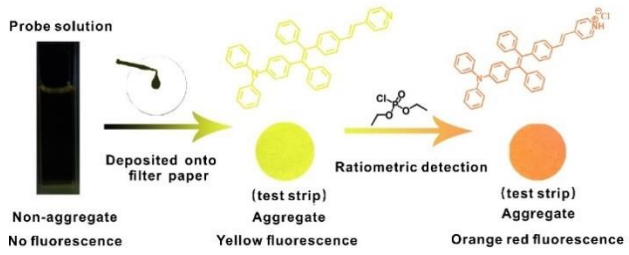

Scheme 1. Schematic illustration of the preparation of DPA-TPE-Py loaded test strips and the detection of DCP. Photographs of the test strips were taken under hand-held UV lamps (365 nm).

solid-state sensors for gas-phase nerve agents[29-31] are all based on fluorophores with aggregation-caused quenching (ACQ)[32,33] properties, which will lead to the reduction of their fluorescence intensities in the solid state and involve certain complex preparation processes, thus seriously eroding the sensors' performance. Contrarily, fluorophores with aggregation-induced emission (AIE)[34-36] properties are very weakly emissive in dilute solution but become highly emissive while forming aggregates due to the restricted intramolecular rotation/vibration[37-40]. Hence AIE probes hold better potential to be developed as portable solid-state sensors than ACQ fluorescent probes due to their intrinsic advantageous feature. Thus, it is highly desirable to develop easily-fabricated and portable solid-state test-strip type AIE fluorescent sensors for ratiometric detection of gas-phase nerve agents. To this end, in this study we have successfully developed a portable sensor DPA-TPE-Py for ratiometric fluorescent detection of diethyl chlorophosphate (DCP) vapors in the form of a paper strip, which is conducive to convenient point-of-use detection, as shown in Scheme 1. Tetraphenylethylene (TPE) has typical aggregation-induced emission (AIE) properties, which is highly emissive in the solid state. In addition, by employing the electron-donor diphenylamine and the electron-acceptor pyridine, we incorporated the push-pull electronic structure into the TPE fluorophore matrix, so as to fabricate the fluorescent probe for responding towards DCP as well as reducing background interference by red-shifting the excitation and/or emission bands of the fluorophore TPE; the probe molecules (DPA-TPE-Py) were deposited onto filter paper to afford the sensor test strip, since filter paper has better gas permeability. As the reactive group and the electron acceptor, pyridine (Py) group is capable of nucleophilically attacking the strong electrophilic phosphonyl group of DCP, resulting in the change of fluorescent signal eventually. To the best of our knowledge, this is the first AIE-probe based paper-strip sensor for rapid ratiometric fluorescent detection of DCP, with the detection limit down to 1.82 ppb level, which is lower than the reported Immediately Dangerous to Life or Health concentration of sarin (7 ppb)[41].

Experimental

View Article Online
DOI: 10.1039/C6TC03116A

Reagents and Materials

(4-Bromo-phenyl)-phenyl-methanone, zinc powder, titanium tetrachloride (GR), tetrahydrofuran (THF for HPLC), diphenylamine, potassium carbonate, palladium acetate, tri-tert-butylphosphine, toluene, triphenylphosphine, 4-vinyl-pyridine, triethylamine, sodium bicarbonate and sodium sulfate were purchased from Aladdin and used as received. Py-COOH, diethyl chlorophosphate (DCP), triethyl phosphate (TEP), tributyl phosphate (TBP), dimethyl methylphosphonate (DMMP) and pinacolyl methylphosphonate (PAMP) were purchased from Sigma-Aldrich. The Whatman qualitative filter paper (Grade 2 1002-070) was purchased from Hangzhou Wohua Co., Ltd. Dichloromethane, hexane, methanol and other solvents were analytically pure reagents and distilled before use. Water used herein was the triple-distilled water upon being further treated with ion exchange columns and a Milli-Q water purification system.

Synthesis of 1, 2- bis(4-bromophenyl)-1,2-diphenylethene (Br-TPE-Br)

Under dry nitrogen atmosphere, (4-bromo-phenyl)-phenyl-methanone (5.22 g, 20 mmol) was added into a 250 mL two-neck round-bottom flask and dissolved in anhydrous THF (120 mL). Subsequently, zinc dust (3.90 g, 60 mmol) was added to the flask, followed by cooling down with an ice bath. Then, $TiCl_4$ (3.30 mL, 30 mmol) was injected into the mixture dropwise. The reaction mixture was stirred and refluxed at 70 °C overnight. After cooling to room temperature, the solvent tetrahydrofuran was evaporated in vacuo and the saturated sodium bicarbonate solution was added until no bubbles came out. Then the mixture was extracted with ethyl acetate three times and dried with anhydrous sodium sulfate. The crude product was purified on a silica-gel column using hexane/dichloromethane (v/v 25:1) as eluent, affording the white solid (4.39 g, 89.6 % yield). ^{1}H NMR (600 MHz, $CDCl_3$, δ ppm):7.08-7.10 (m, 12H), 7.03 (m, 4H), 7.02 (d, J = 1.9 Hz, 2H). MALDI-TOF MS: 487.9496.

Synthesis of {4-[2-(4-bromo-phenyl)-1, 2-diphenyl-vinyl]-phenyl}-diphenyl-amine (DPA-TPE-Br)

A two-neck round-bottomed flask with a reflux condenser was purged with dry nitrogen gas, and Br-TPE-Br (2.67 g, 5.45 mmol) was added and dissolved in dry toluene (30 mL). After that, into the flask were placed diphenylamine (460 mg, 2.72 mmol), K_2CO_3 (1.13 g, 8.16 mmol), $Pd(OAc)_2$ (122 mg, 0.54mmol) and $P(t\text{-}Bu)_3$ (1.90 ml, 1.90 mmol). After reflux at 120 °C for 48 h, the reaction mixture was poured into ethyl acetate, washed three times with water. Then the organic layer was separated and dried over anhydrous sodium sulfate. The solvent was removed by evaporation, and the residue was purified on a silica gel column chromatography using hexane/dichloromethane (v/v 15:1). After being dried in vacuum oven, the yellowish green solid was obtained (1.77 g, 56.2 % yield). ^{1}H NMR (600 MHz, $CDCl_3$, δ ppm): 7.20-7.23 (m, 5.4 Hz, 4H), 7.02-7.15 (m, 22H), 6.86 (s, 2H). MALDI-TOF MS: 577.1118.

Synthesis of (4-{1, 2-diphenyl-2-[4-(2-pyridin-4-yl-vinyl)-phenyl]-vinyl}-phenyl)-diphenyl-amine (DPA-TPE-Py)

A Schlenk tube was charged with DPA-TPE-Br (250 mg, 0.43 mmol), $Pd(OAc)_2$ (4.86 mg, 0.02 mmol), PPh_3 (13.6 mg, 0.05 mmol), 4-vinyl-pyridine (69 μL, 0.65mmol) and anhydrous Et_3N (15 mL) one by one. Immediately, the tube was vacuumed and purged with nitrogen gas three times to remove oxygen completely. Afterwards, the suspension was stirred, heated to 100 °C and refluxed for 72 h. After cooling to room temperature, the resultant was dissolved in ethyl acetate, washed with water for three times and dried over anhydrous sodium sulfate. The crude product was purified by silica column chromatography using dichloromethane/methanol (v/v 100:1) to give product DPA-TPE-Py as saffron yellow solid (86.0 mg, 33.1 % yield). ^{1}H NMR (600 MHz, $(CD_3)_2SO$, δ ppm): 8.52 -8.55 (m, 2H), 7.50-7.55 (m, 2H), 7.44-7.47 (d, J = 23.0 Hz, 2H), 7.26-7.29 (d, J = 13.9 Hz, 2H), 7.23-7.25 (d, J = 7.9 Hz, 2H), 7.07-7.22 (m, 8H), 6.93-7.07 (m, 12H), 6.87-6.90 (d, J = 10.2 Hz, 1H), 6.84 (s, 1H), 6.70-6.74 (m, 2H). ^{13}C NMR (150 MHz, $CDCl_3$, δ ppm): 149.8, 147.5, 146.2, 143.5, 139.9, 137.6, 132.2, 132.0, 131.4, 129.1, 128.9, 127.8, 127.7, 127.1, 126.4, 124.4, 124.3, 122.9, 122.8, 122.5, 121.0. MALDI-TOF MS: 602.2405.

Characterization

^{1}H and ^{13}C NMR spectra were measured with Bruker Avance 600 MHz NMR Spectrometer. MALDI-TOF mass spectra were obtained by using Waters SYNAPT G2-Si high resolution mass spectrometer. UV-vis spectra were measured on a Hitachi U-3010 UV-vis spectrophotometer. Fluorescence spectra were measured by using a Hitachi F-4600 fluorescence spectrophotometer. The fluorescence lifetime data were obtained by using an Edinburgh Instrument FLS920 fluorescence spectrometer. Quantum chemical calculation was performed at the level of B3LYP/6-31G*[42].

Preparation of DPA-TPE-Py loaded test strips

A volume of 20 μL dichloromethane stock solution of DPA-TPE-Py (10^{-3} M) was dropped on a Whatman filter paper with a diameter of 2 cm and air-dried to easily obtain a portable solid test strip for the detection of nerve agent mimic.

Fluorometric analysis

The DPA-TPE-Py loaded test strips were exposed to varied DCP vapor concentrations for 30 s, and then the fluorescence spectrum changes of the test strips were measured with a fluorimeter (excitation wavelength: 465 nm). For selectivity experiments, the test strips were exposed to 0.377 ppm DCP or other related organophosphorous compounds in equal concentration.

Cell viability assay

In order to examine the cytotoxicity of DPA-TPE-Py, HeLa cells (human cervical cancer cells) were used in the experiment; the cells were incubated in DMEM medium added with 10% fetal bovine serum (FBS), maintained at 37 °C with 5% CO_2 and grown for 24 hours. After the medium was removed with PBS buffer, we used DEME medium with 10% FBS to incubate the HeLa cells with addition of DPA-TPE-Py for another 24 hours. The evaluation result of cytotoxicity for DPA-TPE-Py against the cells was acquired by MTT assay in compliance with ISO 10993-5. In these experiments, for each independent experiment, the assays were performed in eight replicates. And the estimation of cell viability was expressed by the statistical mean and standard deviation.

Quantum Chemical Calculations

All of the simulations were performed using the Gaussian 09_B01 program package[43]. The geometry optimizations of the dyes were performed using density functional theory (DFT)[44] with Becke's three-parameter hybrid exchange function with Lee-Yang-Parr gradient-corrected correlation functional (B3-LYP functional) and 6-31G* basis set. No constraints to bonds/angles/dihedral angles were applied in the calculations, and all atoms were free to optimize.

Results and discussion

The AIE-active probe DPA-TPE-Py was synthesized (Scheme S1) and deposited onto filter paper to afford the final test strip. The probe compound and the intermediate compounds were characterized by ^{1}H NMR, ^{13}C NMR and MALDI-TOF mass spectrometry (Fig. S1-S7). Upon obtaining the probe, first the optical properties of DPA-TPE-Py were investigated. The absorption spectrum of DPA-TPE-Py is shown in Fig. S8, and it can be seen that DPA-TPE-Py has absorption at 300-500 nm. The AIE property of DPA-TPE-Py was investigated and compared with a commonly-used non-AIE fluorophore such as Py-COOH. Fig. S9 demonstrates that I_{solid}/I_{liquid} of DPA-TPE-Py at the maximum emission reaches up to 916, while that of the ACQ fluorophore Py-COOH is as low as 0.144; the inset picture also obviously indicates that DPA-TPE-Py does have AIE property. It is obvious that, the emission of ACQ fluorophore is quenched significantly in the solid state, while that of the AIE-

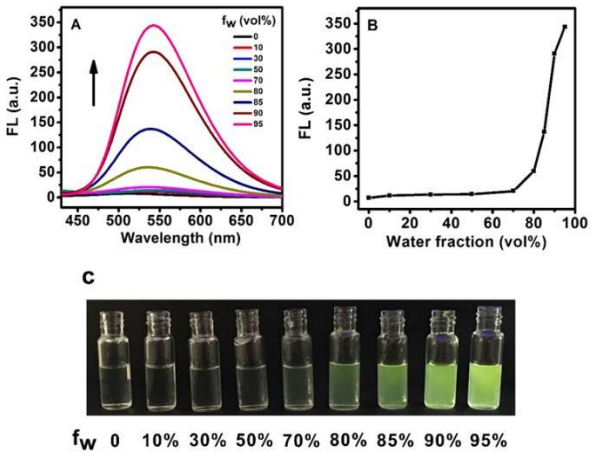

Fig. 1. (A) Fluorescence spectra of DPA-TPE-Py (50 μM) in THF/water mixture (f_w represents water fraction); λ_{ex} =369 nm; (B) Fluorescence intensity of DPA-TPE-Py (50 μM) at 546 nm as a function of water fraction under 369 nm excitation; (C) Photographs of DPA-TPE-Py in THF/water mixture under 365 nm UV light.

active fluorophore is enhanced greatly in the solid state. These results further prove that AIE-active fluorophores hold much greater potential to serve as high-performance solid-state sensors. Also, as shown in Fig. S10, DPA-TPE-Py shows little cytotoxicity against HeLa cells.

The AIE behavior of DPA-TPE-Py was further studied by measuring its fluorescence (FL) spectra in THF/water mixture with different water fractions (Fig. 1), which is a widely used method for evidence of AIE[34-40]. Upon addition of water, the extremely poor solvent for DPA-TPE-Py, aggregates gradually form and the emission at 546 nm enhances with the increasing water fraction. Although the fluorescence intensity of DPA-TPE-Py remains about the same with the water fractions ranging from 0 to 70 vol %, it increases rapidly with further increasing water fractions especially above 80%. Besides, the photostability of DPA-TPE-Py was investigated (Fig. S11). It is clear that, under continuous illumination of daylight and at 15W 365 nm hand-held UV lamp respectively for 2 h, there has been almost no fluorescence intensity loss for DPA-TPE-Py, indicating the advantageous photostability of DPA-TPE-Py. The strong fluorescence emission of DPA-TPE-Py in aggregation state is mainly due to the restriction of intramolecular motion and such a good AIE property of DPA-TPE-Py facilitates its use as portable membrane, sheet or strip sensors.

To investigate the practical ratiometric fluorescent detection of DPA-TPE-Py in aggregation state towards nerve agents, we chose DCP as a mimic analyte. Then we monitored the fluorescence changes of DPA-TPE-Py loaded test strips without or with exposure to different concentrations of DCP for 30 s at 25 °C by fluorescent spectra as shown in Fig. 2A-B. It can be seen that, without exposure to DCP, the DPA-TPE-Py test strip has the maximum fluorescence emission peak at 546 nm, while the emission peak eventually red-shifts to 624 nm upon exposure to DCP. As the DCP level increases, the yellow emission intensity centering around 546 nm of DPA-TPE-Py decreases and in the meantime gradually red-shifts, while the

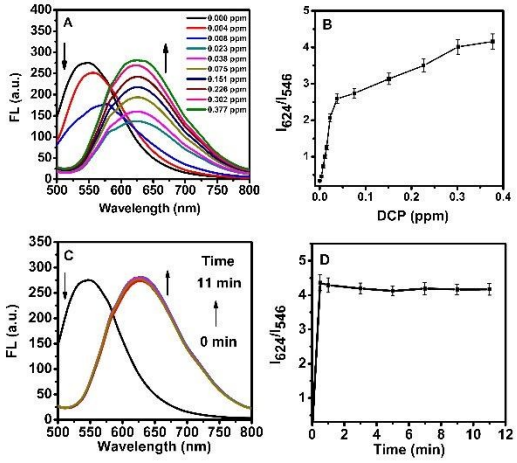

Fig. 2. (A) Fluorescence emission spectra of DPA-TPE-Py loaded test strips upon exposure to different DCP concentrations for 30 s and (B) fluorescence intensity ratio as a function of DCP concentration. (C) Time-dependent fluorescence emission spectra and (D) fluorescence intensity ratio as a function of time upon exposure to 0.377 ppm DCP. Excitation wavelength: 465 nm.

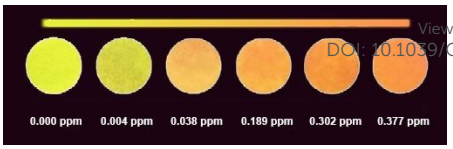

Fig. 3. The photographs of DPA-TPE-Py loaded test strips treated with different DCP vapor concentrations for 30 s at 25 °C taken under 365 nm UV light.

red-shifted orange red emission intensity of the reaction product centering around 624 nm gradually enhances. Upon exposure to increasing DCP levels, the test strips show the maximum emission band red-shifting gradually from 546 nm to 624 nm due to the gradually increasing amount of the product DPA-TPE-PyH from the reaction between DPA-TPE-Py and DCP as well as the different aggregation states of DPA-TPE-Py and the reaction product. Thereby, this handy DPA-TPE-Py loaded test strips can detect DCP levels in a ratiometric way. And the detection limit for DCP vapor has been determined to be 1.82 ppb (Fig. S12). Also, the fluorescence spectra were periodically recorded during different exposure time periods of DPA-TPE-Py loaded test strips to DCP at 0.377 ppm at 25 °C, and the results are shown in Fig. 2C-D. Upon exposure to 0.377 ppm DCP for 30 s, the emission of DPA-TPE-Py decreases, while that of the reaction product increases rapidly. Meanwhile, the fluorescence intensity ratio I_{624}/I_{546} levels off with increased

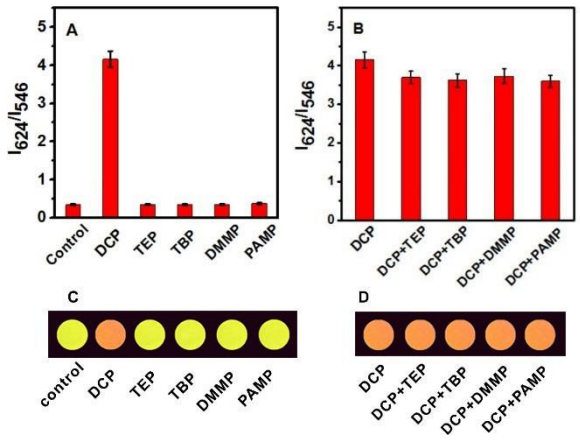

Fig. 4. Fluorescence intensity ratio (I_{624}/I_{546}) of DPA-TPE-Py loaded test strips (A) upon exposure to 0.377 ppm DCP, TEP, TBP, DMMP or PAMP respectively, and (B) exposure to 0.377 ppm DCP, simultaneously in the presence of TEP, TBP, DMMP or PAMP respectively. All fluorescence intensities were measured 30 s after exposure. Excitation wavelength: 465 nm. Photographs of DPA-TPE-Py loaded test strips upon (C) exposure to 0.377 ppm DCP, TEP, TBP, DMMP or PAMP respectively and (D) exposure to 0.377 ppm DCP, simultaneously in the presence of TEP, TBP, DMMP or PAMP in equal concentration respectively were taken under 365 nm UV light.

View Article Online
DOI: 10.1039/C6TC03116A

incubation time from 0.5 min to 11 min. These results clearly demonstrate that DPA-TPE-Py loaded test strips can serve as portable and fast-responding ratiometric fluorescence sensors for DCP vapor detection.

Furthermore, we took photos of the test strips exposed to different concentrations of DCP under a 365 nm handheld UV lamp for direct intuitive observation. And as seen from the photographs (Fig. 3), DPA-TPE-Py loaded on the filter paper itself displays yellow fluorescence, but emits orange red fluorescence gradually after exposure to increasing DCP vapor concentrations. The result demonstrates that, as a handy AIE ratiometric fluorescent sensor for DCP, DPA-TPE-Py loaded test strips are feasible which can act as portable point-of-use test-strip detector for nerve gases.

To study the selectivity of the test-strip sensor, we tested such possible interfering species as triethyl phosphate (TEP), tributyl phosphate (TBP), dimethyl methylphosphonate (DMMP) and pinacolyl methylphosphonate (PAMP) in parallel under the same conditions. As seen in Fig. 4A and C, the fluorescence intensity ratio I_{624}/I_{546} induced by DCP is much higher than those possible interferents and only the DPA-TPE-Py loaded test strip treated with DCP vapor has changed from yellow to orange red, indicating that DPA-TPE-Py is quite a sensitive and selective probe for DCP detection. Also, we examined the detection of DPA-TPE-Py for DCP in the presence of the above possible interferents. And it can be seen from Fig. 4B and D that the co-existence of these species has little interfering effect on DCP detection.

The schematic illustration for the proposed ratiometric fluorescent response of the test strip toward DCP is shown in Fig. 5. In the molecular structure of DPA-TPE-Py, the pyridine group has stronger nucleophilicity (pKa = 5.17) and smaller steric hindrance compared with the diphenylamine group (pKa = 1.20). Hence, the pyridine group will be first electrophilically attacked by the phosphonyl group of DCP, forming the unstable intermediate, whose N-P bond is easily further attacked by weak nucleophilic reagent like oxygen atom from H_2O vapor and ultimately be rapidly hydrolyzed into pyridinium salt, namely the reaction product DPA-TPE-PyH. As a result of the enhanced push-pull electron effect, obvious fluorescenct changes at two different wavelengths can be observed. Meanwhile, the nerve agent mimic DCP will transform into non-toxic neutral phosphate. That is, ratiometric fluorescent detection for DCP can be effectively realized by this way.

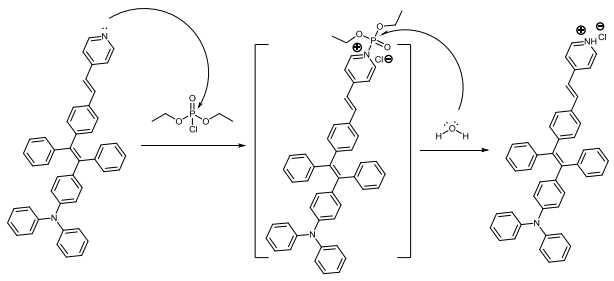

Fig. 5. Proposed mechanism for the ratiometric fluorescent response of DPA-TPE-Py to DCP.

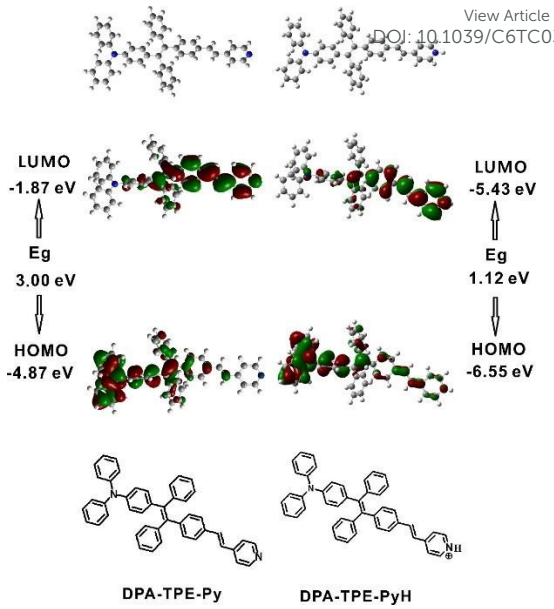

Fig. 6. Optimized molecular structures and molecular orbitals of DPA-TPE-Py and the final reaction product (DPA-TPE-PyH) of DPA-TPE-Py with DCP vapor.

To examine and confirm the proposed response mechanism, ^{1}H NMR and MS measurements were firstly conducted for the product from the reaction between DPA-TPE-Py and DCP. As can be seen from Fig. S13, the molecular weight peak at 603.2478 m/z corresponds to the reaction product DPA-TPE-PyH, which is produced by the reaction of DPA-TPE-Py and DCP. Also, from ^{1}H NMR spectra (Fig. S14 and S15), it is clear that the proton peaks of pyridine moiety had moved significantly from 8.5 and 7.5 to 8.8 and 8.2 respectively upon reaction. Moreover, we measured absorption spectra and fluorescence lifetimes for the test strips before and after reacting with DCP. It is obvious that, the maximum absorption (Fig. S8) and emission peaks (Fig. 2) of the reaction product DPA-TPE-PyH were red-shifted compared with the probe DPA-TPE-Py. Also, the lifetime of DPA-TPE-PyH measured at 624 nm (emission) were 0.80 ns and 3.65 ns, which was different from 1.10 ns and 3.45 ns of DPA-TPE-Py measured at 546 nm (emission) (Fig. S16).

To further prove the detection mechanism, as for DPA-TPE-Py and its reaction product DPA-TPE-PyH, and their frontier molecular orbital (FMO) energies were calculated using Gaussian 09 (DFT in B3LYP/6-31G* level). It can be seen in Fig. 6, DPA-TPE-Py has a characteristic of intramolecular charge transfer at its excited state. The electron is delocalized on DPA in its HOMO (-4.87 eV), while delocalized on the pyridine unit and the phenyl of the TPE ring connected with it in its LUMO (-1.87 eV). Compared with DPA-TPE-Py, the reaction product DPA-TPE-PyH, whose pyridine group was protonated, has a lower HOMO (-6.55 eV) and LUMO (-5.43 eV). In addition, the energy gap (E_g) of DPA-TPE-PyH was calculated to be 1.12 eV, lower than that of DPA-TPE-Py (3.00 eV). The lower E_g of DPA-TPE-PyH indicates a stronger intramolecular charge transfer

process, further resulting in absorption and emission peak red-shifts. The results of theoretical calculations by Gaussian 09 was consistent with our experimental results, suggesting that our proposed response mechanism is reasonable.

Conclusions

In summary, we have developed a novel AIE fluorophore (DPA-TPE-Py) based test-strip sensor for ratiometric fluorescence detection of gaseous nerve agent mimic DCP in a rapid, sensitive and selective way. The fluorophore exhibits strong emission in the aggregated state, which is conducive to the solid test-strip sensing; also it has quite good photostability, which is in favour of applications in the long term. Moreover, the handy and portable DPA-TPE-Py loaded solid test strips are easy to prepare by direct deposition of the probe molecules onto the filter paper. The pyridine group of DPA-TPE-Py turns into pyridinium group after reaction with DCP vapor, resulting in an emission spectral red-shift from 546 nm to 624 nm. The change in fluorescence of DPA-TPE-Py loaded test strips upon contact with DCP can be clearly observed by naked eye by the aid of a portable UV lamp. The detection limit is determined to be as low as 1.82 ppb. The strategy herein will be helpful for devising convenient ratiometric fluorescent sensors in solid state and providing a portable approach for detection of gaseous nerve agents.

Acknowledgements

We gratefully acknowledge the financial support by the Science and Technology Planning Project of Guangzhou (Project No. 201607020015), the National Key Basic Research Program of China (Project No. 2013CB834702), NSFC (21574044, 21474031 and 51673066), the Natural Science Foundation of Guangdong Province (2016A030312002) and the Fundamental Research Funds for the Central Universities (2015ZY013). The authors greatly appreciate the help of Dr. Xinyi Cai with theoretical calculations and discussions.

Notes and References

1 H. J. Kim, J. H. Lee, H. Lee, J. H. Lee, J. H. Lee, J. H. Jung and J. S. Kim, *Adv. Funct. Mater.*, 2011, **21**, 4035.
2 V. V. Singh, K. Kaufmann, B. E. de Ávila, M. Uygun and J. Wang, *Chem. Commun.*, 2016, **52**, 3360.
3 A. Balamurugan and H. Lee, *Macromolecules*, 2016, **49**, 2568.
4 M. R. Sambrook and S. Notman, *Chem. Soc. Rev.*, 2013, **42**, 9251.
5 J. G. Weis and T. M. Swager, *ACS Macro Lett.*, 2015, **4**, 138.
6 A. D. Rusu, I. A. Moleavin, N. Hurduc, M. Hamel and L. Rocha, *Chem. Commun.*, 2014, **50**, 9965.
7 J. Yao, Y. Fu, W. Xu, T. Fan, Y. Gao , Q. He, D. Zhu, H. Cao and J. Cheng, *Anal. Chem.*, 2016, **88**, 2497.
8 K. Kim, O. G. Tsay, D. A. Atwood and D. G. Churchill, *Chem. Rev.*, 2011, **111**, 5345.
9 W. Wu, J. Dong, X. Wang, J. Li, S. Sui, G. Chen, J. Liu and M. Zhang, *Analyst,* 2012, **137**, 3224.
10 M. G. Caglayan, S. Sheykhi, L. M. Mosca and P. Anzenbacher Jr, *Chem. Commun.*, 2016, **52**, 8279. View Article Online DOI: 10.1039/C6TC03116A
11 X. Chen, F. Wang, J. Y. Hyun, T. Wei, J. Qiang, X. Ren, I. Shin and J. Yoon, *Chem. Soc. Rev*., 2016, **45**, 2976.
12 J. Ding, H. Li, C. Wang, J. Yang, Y. Xie, Q. Peng, Q. Li and Z. Li, *ACS Appl. Mater. Interfaces*, 2015, **7**, 11369.
13 X. He, Y. Zang, T. D. James, J. Li and G. Chen, *Chem. Soc. Rev*., 2015, **44**, 4239.
14 V. S. Lin, W. Chen, M. Xian and C. J. Chang, *Chem. Soc. Rev.*, 2015, **44**, 4596.
15 P. Li, L. Liu, H. Xiao, W. Zhang, L. Wang and B. Tang, *J. Am. Chem. Soc*., 2016, **138**, 2893.
16 C. Zhao, X. Zhang, K. Li, S. Zhu, Z. Guo, L. Zhang, F. Wang, Q. Fei, S. Luo and P. Shi, *J. Am. Chem. Soc*, 2015, **137**, 8490.
17 S. U. Hettiarachchi, B. Prasai and R. L. McCarley, *J. Am Chem Soc*, 2014, **136**, 7575.
18 M. H. Lee, J. S. Kim and J. L. Sessler, *Chem. Soc. Rev*., 2015, **44**, 4185.
19 H. Zhang, M. Cao, W. Wu, H. Xu, S. Cheng and L. Fan, *Nanoscale*, 2015, **7**, 1374.
20 L. A. Juárez, A. M. Costero, M. Parra, S. Gil, F. Sancenón and R. Martínez-Máñez, *Chem. Commun.*, 2015, **51**, 1725.
21 C. Yu, X. Li, F. Zeng, F. Zheng and S. Wu, *Chem. Commun.*, 2013, **49**, 403.
22 S. I. Reja, I. A. Khan, V. Bhalla and M. Kumar, *Chem. Commun.*, 2016, **52**, 1182.
23 S. Shen, X. Chen, X. Zhang, J. Miao and B. Zhao, *J. Mater. Chem. B*, 2015, **3**, 919.
24 Y. Wu, J. Wang, F. Zeng, S. Huang, J. Huang, H. Xie, C. Yu and S. Wu, *ACS Appl. Mater. Interfaces*, 2016, **8**, 1511.
25 D. Pangeni and E. E. Nesterov, *Macromolecules*, 2013, **46**, 7266.
26 B. Diaz De Grenu, D. Moreno, T. Torroba, A. Berg, J. Gunnars, T. Nilsson, R. Nyman, M. Persson, J. Pettersson and I. Eklind, *J. Am. Chem. Soc*., 2014, **136**, 4125.
27 X. Hu, Y. Su, Y. Ma, X. Zhan, H. Zheng and Y. Jiang, *Chem. Commun.*, 2015, **51**, 15118.
28 S. Jo, D. Kim, S. Son, Y. Kim and T. S. Lee, *ACS Appl. Mater. Interfaces*, 2014, **6**, 1330.
29 X. Zhou, Y. Zeng, L. Chen, X. Wu and J. Yoon, *Angew. Chem., Int. Ed.*, 2016, **55**, 4729.
30 S. Sarkar and R. Shunmugam, *Chem. Commun.*, 2014, **50**, 8511.
31 W. Xuan, Y. Cao, J. Zhou and W. Wang, *Chem. Commun*., 2013, **49**, 10474.
32 Y. Wu, S. Huang, F. Zeng, J. Wang, C. Yu, J. Huang, H. Xie and S. Wu, *Chem. Commun.*, 2015, **51**, 12791.
33 J. Wang, Y. Wu, F. Zeng, S. Huang, and S. Wu, *Faraday Discuss*., 2016, DOI: 10.1039/C6FD00118A.
34 Z. Song, W. Zhang, M. Jiang, H. H. Sung, R. T. Kwok, H. Nie, I. D. Williams, B. Liu and B. Z. Tang, *Adv. Funct. Mater.*, 2016, **26**, 824.
35 A. Shao, Y. Xie, S. Zhu, Z. Guo, S. Zhu, J. Guo, P. Shi, T. D. James, H. Tian and W. H. Zhu, *Angew. Chem., Int. Ed.*, 2015, **54**, 7275.
36 H. Wang, D. Chen, Y. Zhang, P. Liu, J. Shi, X. Feng, B. Tong and Y. Dong, *J. Mater. Chem. C.*, 2015, **3**, 7621.
37 F. Hu, G. Zhang, C. Zhan, W. Zhang, Y. Yan, Y. Zhao, H. Fu and D. Zhang, *Small,* 2015, **11**, 1335.
38 Y. Gao, G. Feng, T. Jiang, C. Goh, L. Ng, B. Liu, B. Li, L. Yang, J. Hua and H. Tian, *Adv. Funct. Mater.*, 2015, **25**, 2857.
39 H. Lu, Y. Zheng, X. Zhao, L. Wang, S. Ma, X. Han, B. Xu, W. Tian and H. Gao, *Angew. Chem., Int. Ed.*, 2016, **128**, 163.
40 Z. Guo, A. Shao and W. Zhu, *J. Mater. Chem. C.*, 2016, **4**, 2640.
41 R. H. Kagann, R. A. Hashmonay and D. B. Harris, Annual Meeting of the Air & Waste Management Association, 2005.
42 P. Zhao, L. Xu, J. Huang, K. Zheng, B. Fu, H. Yu and L. Ji, *Biophys. Chem.*, 2008, **135**, 102.

View Article Online
DOI: 10.1039/C6TC03116A

43 M. J. Frisch, G. W. Trucks, H. B. Schlegel, G. E. Scuseria, M. A. Robb, J. R. Cheeseman, G. Scalmani, V. Barone, B. Mennucci and G. A. Petersson, *Gaussian Inc., Wallingford, CT*, 2009.
44 R. M. Dreialer and E. Gross, Density Functional Theory: An Approach to Quantum Many Body Problem, Springer: Berlin, Germany, 1990.

View Article Online
DOI: 10.1039/C6TC03116A

Table of Contents

The first AIE-probe based paper-strip sensor for rapid and point-of-use fluorescent detection of gaseous nerve agent mimic has been developed.